

LAMINAR AND TURBULENT HEAT TRANSFER IN THE PIPE ENTRANCE REGION FOR LIQUID METALS

CHING-JEN CHEN and JENQ SHING CHIOU†

Energy Division and Iowa Institute of Hydraulic Research, University of Iowa, Iowa City, IA 52242, U.S.A.

(Received 8 July 1980 and in revised form 8 January 1981)

Abstract—Laminar and turbulent heat transfer in the pipe flow for liquid metals are studied. Three flow regions, namely fully developed, developing thermal, and developing thermal and velocity regions, are considered. The modified van Driest and Cebeci mixing length turbulence model is adopted in the analysis. The thermal damping constant is redetermined in the study for the fully-developed region as well as other developing regions. The predicted results are compared with experimental data when available. Correlation for heat transfer calculation is given for boundary conditions of constant heat flux and constant wall temperature. The effect of the variation of physical properties is also studied. Correlation of heat transfer calculation when the property is variable is given in a simple form for liquid sodium and NaK eutectic.

NOMENCLATURE

A ,	cross-section area;
A^+ ,	momentum damping coefficient;
B^+ ,	thermal damping coefficient;
B_{∞}^+ ,	thermal damping coefficient for the fully-developed region;
C_i ,	empirical constants, equation (2);
C_p ,	specific heat at constant pressure;
D ,	diameter;
E, F ,	constants in equation (25) and (26);
g ,	square of fluctuating temperature;
L ,	axial length;
l ,	mixing length;
K ,	Karman constant;
K' ,	thermal turbulent constant;
k ,	turbulent kinetic energy, or thermal conductivity;
k_t ,	turbulent thermal conductivity;
Nu_x ,	local Nusselt number $h_x D/k$;
Nu_{∞} ,	fully-developed Nusselt number;
Pe ,	Peclet number, $RePr$;
P ,	pressure;
Pr ,	Prandtl number;
Pr_t ,	turbulent Prandtl number;
q_w ,	local wall heat flux;
Re ,	Reynolds number $\bar{U}D/\nu$;
R ,	radius of tube;
r ,	radial coordinate;
u^* ,	friction velocity, $\sqrt{(\tau_w/\rho)}$;
u ,	axial velocity component;
v ,	radial velocity component;
x ,	axial direction;
y ,	$y = R - r$;
y^+ ,	yu^*/ν dimensionless distance.

Greek symbols

τ_w ,	local wall shear stress;
μ ,	molecular viscosity;
μ_t ,	turbulent eddy viscosity;
ϵ ,	turbulent dissipation function;
ρ ,	density;
δ_T ,	enthalpy boundary layer;
λ ,	0.09 constant;
ζ ,	$(x/D)/Pe$ local Graetz number.

Indices

eff,	effective;
t ,	turbulent or thermal;
$[\bar{n}]$,	mean;
∞ ,	fully developed;
x ,	local;
m ,	mean;
w ,	wall;
ϕ ,	center line;
i ,	inlet;
q ,	constant wall heat flux;
b ,	bulk;
f ,	film;
T ,	constant wall temperature.

1. INTRODUCTION

LIQUID metal heat transfer has been a subject of interest for more than thirty years. This is because liquid metals, in general, possess large thermal conductivity, small kinematic viscosity, small vapor pressure and an extensive temperature range over which they remain in the liquid phase. These characteristics make liquid metal especially valuable for certain important uses. The most familiar application is their use as coolants for the liquid metal fast breeder reactor. They are also the potential working fluids for situations where the heat-exchange surface is limited but a large heat-transfer rate is still desired, such as in a space power plant.

† Present address: Nuclear Safety Department, Westinghouse Research Center, Monroeville, PA 15146, U.S.A.
 © 1981 U.S. Government.

Liquid metals, although they behave as Newtonian fluids, have very high thermal diffusivity and very low kinematic viscosity. Thus the Prandtl number is of low order, 10^{-2} . An important consequence of the low value of the Prandtl number is that in turbulent flows the molecular heat transport is important not only in the viscous sublayer region, but also in the buffer zone and even in some parts of turbulent regions. Physically this means that thermal diffusion from the wall boundary can penetrate much deeper into the turbulent region in liquid metals than would be possible in ordinary fluids. Consequently, thermal boundary conditions have a strong influence on heat-transfer characteristics in liquid metal flows. Most of the past solutions of turbulent heat transfer in a circular tube had concentrated on a flow which is fully developed, whose physical properties are constant, and whose wall boundary is either at isothermal or constant heat flux conditions. In this study, heat transfer in pipe flow is investigated not only for the fully-developed region, but also for the developing thermal region and the developing thermal and velocity region. In addition, the physical properties of the liquid metals are considered to be variable, being a function of temperature, and the wall boundary is specified either by a temperature or by a heat flux distribution. The numerical solutions are obtained from the modified Patankar–Spalding [1] computer code. The van Driest [2] mixing length hypothesis is adapted to model the turbulent shear stress, and the Cebeci model [3] is extended to model the turbulent thermal conductivity of liquid metal flows.

2. TURBULENT MODEL AND HEAT-TRANSFER CORRELATION

The mixing length model of turbulent momentum transfer for liquid metal is the same as for ordinary fluids and is relatively well developed for pipe flows. However, the modeling of turbulent energy transport for liquid metals is not well developed, partly because the experimental data are scarce and partly because an accurate experiment is difficult to perform. Jenkins [4], Deissler, [5], Azer and Chao [6] and Dwyer [7] modified the Prandtl mixing length model in which the turbulent eddy is considered to be a heat conducting sphere possessing a high thermal diffusivity. They all proposed a model of the turbulent Prandtl number which provides a functional link between turbulent momentum diffusivity and turbulent thermal diffusivity. Cebeci [3] recently adopted van Driest's idea of near-wall damping of the mixing length to propose the turbulent Prandtl number as

$$Pr_t = \frac{K[1 - \exp(-y'/A^+)]}{K'[1 - \exp(-y^+ \sqrt{(Pr)/B^+})]} \quad (1)$$

where K is the Karman constant and K' is the constant for the thermal mixing length. A^+ and B^+ are the damping coefficients for momentum and thermal mixing length, respectively. $y^+ = yu^*/\nu$ is the distance, y , from the wall normalized by the friction velocity u^*

$= \sqrt{(\tau_w/\rho)}$ and the kinematic viscosity ν . Na and Habib [8] extended the Cebeci [3] model for liquids of lower Prandtl number by setting $K = K'$ and proposed the damping constant B^+ as

$$B^+ = \sum_{i=1}^5 C_i (\log_{10} Pr)^{i-1} \quad 0.02 \leq Pr \leq 15 \quad (2)$$

where C_i s are empirical constants. The range of Prandtl numbers given in equation (2) is not sufficient to cover all liquid metals. Equation (2) was also found in this study to be inaccurate in the lower range of Prandtl numbers. We redetermine the damping coefficient B^+ for liquid metals with the more accurate data of Nusselt number correlation obtained by Baker and Sesonske [9], Subbotin *et al.* [10] and Borishanskii and Kutatedadze [11].

In addition to the mixing length model, there are turbulence models to solve directly the turbulence stresses and turbulent heat fluxes by their respective turbulent transport equations. For example, Sha and Launder [12] proposed a turbulence model for liquid metal based on three differential scalar equations. The three scalar quantities are turbulent kinetic energy k ; turbulent energy dissipation rate ε ; and turbulent temperature g . The other turbulent transport quantities are then obtained from the approximated algebraic equations. In the k - ε - g turbulence model, the near wall region also required special treatment because of its strong nonisotropic behavior and the influence of the laminar sublayer. Although the high-order turbulence model potentially has wider application, than mixing length model, use of such models for liquid metals requires further study. On the other hand, for simple geometries such as the circular tube, Stephenson [13] showed that the mixing length model is as good as the k - ε model for developing air flows. The difference is that the k - ε turbulence model, unlike the mixing length model, predicts a peak axial velocity in the entrance region before the velocity profile reaches the fully-developed state. In this paper a modified mixing length model is adopted.

From an engineering point of view, the gross heat transfer coefficient is of great interest. Therefore many empirical or semi-empirical formulae for evaluating the value of Nusselt numbers [14–18] have been proposed. In the fully-developed flow region, Martinelli [14] and Lyon [15] analyzed turbulent heat transfer in a circular tube under a constant wall heat flux condition. Lyon gave a semi-empirical expression for the fully-developed pipe flow as

$$Nu = 7 + 0.025 (Pr_t^{-1} Pe)^{0.8}. \quad (3)$$

This is the well-known Martinelli–Lyon equation for liquid metals [15]. Lubarsky and Kaufman [16] re-evaluated the available past experimental data in the developed region and proposed that the Nusselt number should be

$$Nu = 0.625 Pe^{0.4}. \quad (4)$$

This formula gives values of Nusselt numbers 30%

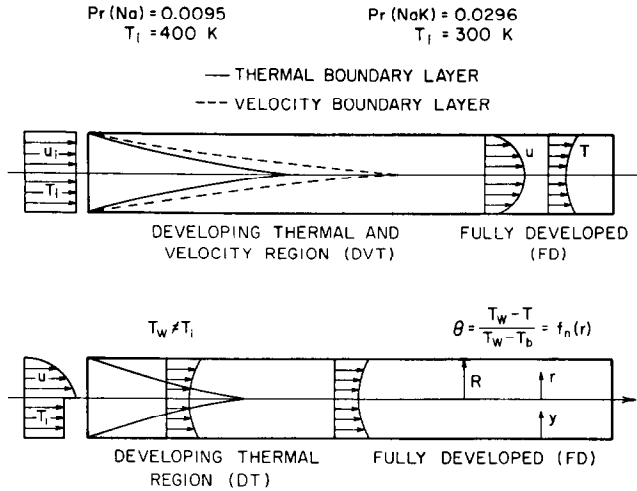


FIG. 1. Regions and coordinates.

below those of equation (3). Many later proposals, such as Dwyer [17] and Sleicher, Awad and Natter [18], suggested a Nusselt number formula with a value that falls in the region between equation (3) and (4). According to the experiments of Subbotin *et al.* [10], Baker and Sesonske [9], and Borishanskii and Kutateladze [11], the Nusselt number of turbulent liquid metal flow in the fully-developed region of circular tube should indeed be between equation (3) and (4). The suggested Nusselt number correlation for experimental data will be given later.

In the entrance region, the experimental data or predicted Nusselt numbers are rather limited. Awad [19] measured the NaK eutectic heat transfer coefficient at several locations along the axial direction of a circular pipe. Later, Sleicher, Awad and Natter [18] proposed an approximate empirical formula for the developing thermal (DT) region as

$$Nu_x = Nu_\infty \left(1 + \frac{2}{x/D} \right) \text{ for } x/D > 4 \quad (5)$$

where the fully-developed Nusselt number, Nu_∞ , is given as

$$Nu_\infty = 4.8 + 0.0156 Pe^{0.88} Pr^{0.08}$$

for flow with uniform wall temperature; and

$$Nu_\infty = 6.3 + 0.0167 Pe^{0.85} Pr^{0.08}$$

for flow with uniform wall heat flux. In our experimental set-up the turbulent pipe flow was divided into three regions as shown in Fig. 1: the fully-developed region where both velocity and temperature distribution are developed, a developing thermal region where the velocity profile is fully developed but the temperature profile is developing, and the developing thermal and velocity region where both velocity and temperature profiles are developing. New correlations for Nusselt numbers in these regions are given. The

effect of property variation on the Nusselt number is also investigated.

3. ANALYSIS

In order to formulate the problem, the following assumptions are made: (a) the mean flow is steady, turbulent and axisymmetric, (b) body forces are negligible, (c) there is no phase change, (d) physical properties are functions of mean temperature, (e) the Peclet number, $Pe = PrRe$, is larger than 50, such that the axial thermal diffusion is small compared with the radial thermal diffusion and can be neglected; (f) boundary layer approximation is applicable at the entrance region; and (2) the turbulent transport properties are modeled by the eddy viscosity μ_t and thermal conductivity k_t model with van Driest and Cebeci modification of the mixing length approximation. With these assumptions, the governing equations in cylindrical coordinates (Fig. 1) can be written as

$$\frac{\partial(\rho u)}{\partial x} + \frac{1}{r} \frac{\partial}{\partial r} (r \rho v) = 0 \quad (6)$$

$$\rho u \frac{\partial u}{\partial x} + \rho v \frac{\partial u}{\partial r} = - \frac{dP}{dx} + \frac{1}{r} \frac{\partial}{\partial r} \left[r(\mu + \mu_t) \frac{\partial u}{\partial r} \right] \quad (7)$$

$$\rho C_p \left(u \frac{\partial T}{\partial x} + v \frac{\partial T}{\partial r} \right) = \frac{1}{r} \frac{\partial}{\partial r} \left[r(k + k_t) \frac{\partial T}{\partial r} \right] + u \frac{dP}{dx} + \mu \left(\frac{\partial u}{\partial r} \right)^2 + \varepsilon \quad (8)$$

where the pressure gradient dP/dx in equations (7) and (8) may be obtained from the total momentum balance in the axial direction of the pipe as

$$\frac{dP}{dx} = \frac{-2\pi R \tau_w}{A} + u^{-2} \frac{d\bar{\rho}(x)}{dx} \quad (9)$$

Here τ_w is the local wall shear stress, A is the cross-

sectional area, \bar{u} is the mean (or bulk) velocity, and $\bar{\rho}$ is the mean density.

With the van Driest mixing length hypothesis [2] the eddy viscosity may be written as with $y = R - r$

$$\mu_{\text{eff}} = \mu + \mu_t = \mu + \rho l^2 \left| \frac{\partial u}{\partial y} \right| \frac{\partial u}{\partial y}$$

where

$$l = Ky[1 - \exp(-y^+/A^+)] \quad \text{if } 0 < y \leq \frac{\lambda R}{K} \quad (10)$$

$$l = \lambda R \quad \text{if } y > \frac{\lambda R}{K}.$$

In equation (10) R is the radius of the pipe, $\lambda = 0.09$, $K = 0.435$, $A^+ = 26$, $y^+ = yu^*/\nu$, and $u^* = \sqrt{(\tau_w/\rho)}$.

On the other hand, turbulent conductivity k_t is modeled by Cebeci's model [3] or

$$k_{\text{eff}} = k + k_t = k + \rho l_t \left| \frac{\partial u}{\partial y} \right| \frac{\partial T}{\partial y}$$

with l as given in equation (10), and

$$l_t = K'y[1 - \exp(-y^+ \sqrt{Pr/B^+})]. \quad (11)$$

Here Pr is the molecular Prandtl number, K' is a constant, and B^+ is the damping constant of the thermal mixing length. The turbulent Prandtl number $Pr_t = C_p \mu_t / k_t$, derived from equation (10) and (11) is then equal to equation (1). However, instead of equation (2) we propose the value of B^+ to be

$$B^+ = B_\infty^+ \frac{\delta_T}{\delta_{T\infty}} \quad (12)$$

$B_\infty^+ = 10.5 Pr^{-1/3}$, the damping constant for the fully developed region, is determined from experimental data [7-11, 18, 19]. δ_T is the enthalpy thickness and is defined as

$$\delta_T = \frac{\int_0^R \rho u (h_\xi - h) dy}{\rho_\xi u_\xi (h_\xi - h_w)} \quad (13)$$

The subscripts w , ∞ and ξ indicate that the values are evaluated at the wall, the fully-developed region, and the center line of the pipe, respectively.

The initial condition for fluid entering a circular tube is taken to be uniform temperature T_i and velocity distribution u_i or

$$u(0, r) = u_i \quad (14)$$

$$T(0, r) = T_i.$$

The symmetry condition at the center line requires that

$$\frac{\partial u}{\partial r}(x, 0) = 0, \quad v(x, 0) = 0 \quad (15)$$

$$\frac{\partial T}{\partial r}(x, 0) = 0.$$

At the pipe wall, the no-slip and thermal conditions given

$$u(x, R) = 0, \quad v(x, R) = 0 \quad (16)$$

$$T(x, R) = T_w(x) \quad \text{or} \quad \frac{\partial T}{\partial r}(x, R) = \frac{-q_w}{k}.$$

Here q_w is the local heat flux per unit inner surface area. The property equations used in the calculation are taken from data given by Foust [20].

The governing equations (6)-(8) are solved by a modified version of Patankar and Spalding computer code [1]. Basically it is the integral implicit finite-difference numerical scheme. 'Integral' means to integrate the governing equations over a control element therefore the conservation of the dependent variables, such as energy, momentum and mass, is preserved. The main features of the Patankar-Spalding program [1], such as predicted-corrected pressure gradient, reduced von Mises coordinates, and Couette flow assumption near the wall are all adopted in this study, but with several changes. First, the thermal turbulence model given by equation (11) is used for the calculation of energy equation. Secondly, instead of the original near wall enthalpy function proposed by Patankar and Spalding [1] which is valid only for $Pr > 0.5$ the wall temperature function

$$T^+ = \frac{(T - T_w)\rho c_p \bar{u}}{q_w} = Pr y^+ \quad (17)$$

is used for liquid metal flow in the near wall region. Equation (17) is derived from turbulent energy equation (8) under the Couette flow assumption and neglecting the kinetic heating. Eddy thermal conductivity k_t is neglected in the near wall region, since it is small near the wall compared with the extremely large molecular thermal conductivity.

Indeed Kirillov's measurements [21] indicate that molecular thermal diffusion overwhelms turbulent energy transport near the wall. Kirillov's data [21] show that equation (17) is valid for

$$Pr y^+ < 1. \quad (18)$$

That is, for liquid metal with $Pr = 0.01$ the upper bound of y^+ is 100. This is more than sufficient for the present liquid metal calculation near the wall since the near wall regions are normally limited to y^+ less than 50. The third change made is that a value of 0.435 is used for Karman constant (instead of 0.415 used by Patankar and Spalding) so that the friction coefficient for the pipe flow in the fully developed region agrees best with the Prandtl universal law of friction. In this study, 20 to 30 cross-stream nodes were employed in most of the calculations. A forward marching step length of 0.05 or 0.1 diameter was used. To verify the numerical accuracy, several calculations were made with 40 and 60 cross-stream nodes with a step length of 0.025 diameter. In either case the calculated heat transfer and wall friction coefficients are within 1% difference, therefore grid independent results are obtained.

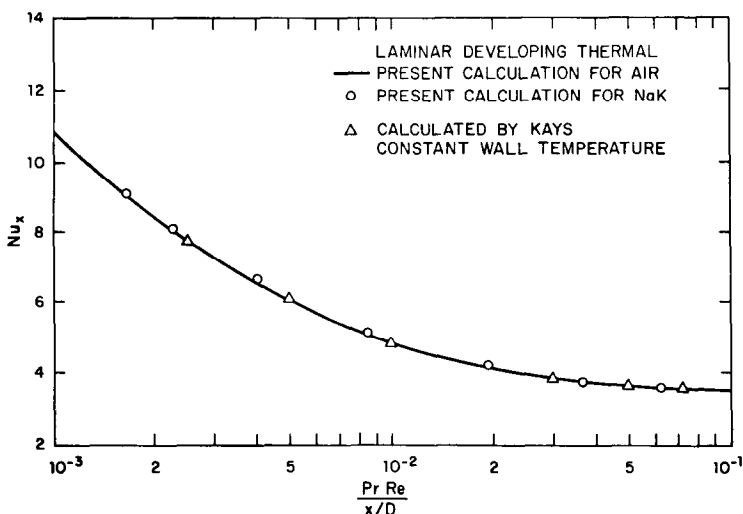


FIG. 2. Laminar heat transfer in developing thermal region.

4. DISCUSSION OF LAMINAR FLOWS

The main purpose of the laminar-flow calculation was to test whether the modified program predicts some known solutions and to discuss any disparity. Figure 2 shows the local Nusselt number $Nu_x = h_x D/k$ vs the inverse Graetz number $\zeta = (x/D)/Pe$ for air and NaK eutectic in the laminar developing thermal (DT) region with isothermal wall boundary condition, a problem known as the Graetz-Nusselt problem. Figure 2 indicates that the predicted results for the local Nusselt number is a function of ζ only. This is consistent with the solution given by Nusselt and Kays [22]. Furthermore, the predicted Nusselt number for the fully-developed (FD) region also agrees with the analytical value of $Nu_{\infty, T} = 3.66$ given by Kays [28]. Figure 3 shows the local Nusselt number, Nu_x , vs the Graetz number ($1/\zeta$) for air and NaK eutectic in the

laminar developing thermal and velocity (DTV) region with a constant wall heat flux. The present prediction, and those by Banston and McEligot [24], McMordie and Emery [25], and Nusselt and Kays [22], all approach the theoretical value of $Nu_{\infty, q} = 4.36$ for the fully-developed flow at far downstream $PrRe/(x/D) < 5$. The present results in the DTV region are consistent with the results of Banston and McEligot [24] for air ($Pr = 0.75$) and also with those of McMordie and Emery [25] for NaK eutectic ($Pr = 0.02$). However, Kays' calculation [23] for air is higher than both the present results and Banston and McEligot's [24].

To explain this disparity let us first compare the results between the developing thermal (DT) region given in Fig. 2, and the developing thermal and velocity (DTV) region given in Fig. 3. The comparison illustrates an interesting point, that the local Nusselt

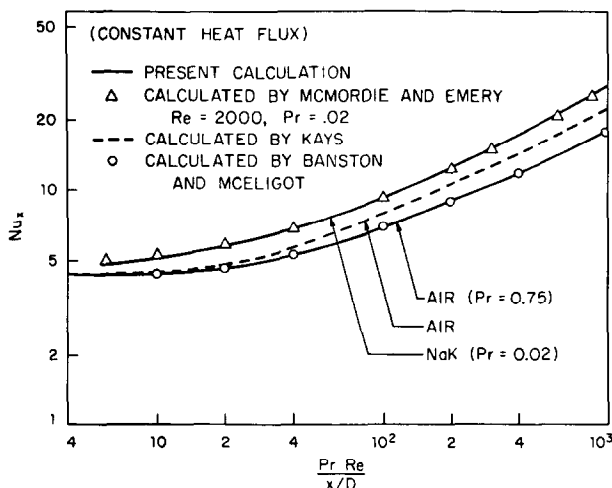


FIG. 3. Laminar heat transfer in developing thermal and velocity region.

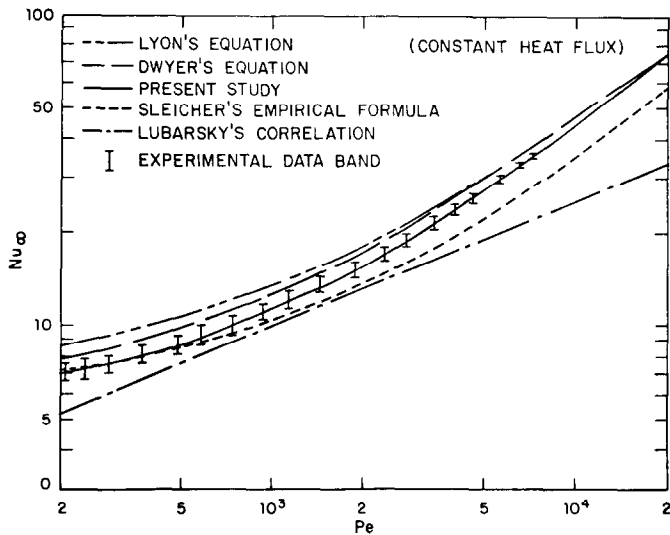


FIG. 4. Turbulent heat transfer in fully-developed region.

number in the DT region is a function of the inverse Graetz number only, while the local Nusselt number in the DTV region depends not only on the inverse Graetz number but also on the Prandtl number. This difference is due to the existence of a radial velocity component in the DTV region. This component disallows the normalization of the governing equation to absorb both Prandtl and Reynolds number into a single independent variable. As a consequence of omitting the radial velocity component in Kays' [22] analysis, the local Nusselt number in the DTV region is a function of the Peclet number only. This explains the disparity between Kays' results and the present or Branston and McEligot's predictions.

5. DISCUSSION OF TURBULENT FLOWS

The results of the present analysis have been obtained for three turbulent flow regions, namely the fully developed (FD) region, the developing thermal

(DT) region, and the developing thermal and velocity (DTV) region.

1. Fully-developed region (FD)

The calculated Nusselt number vs Peclet number in the FD region is first correlated with the experimental data obtained by Baker and Sesonske [9], Subbotin *et al.* [10], Borishanskii and Kutateladze [11]. The thermal damping coefficient B_{∞}^{+} is determined in the fully-developed region as

$$B_{\infty}^{+} = 10.5 Pr^{-1/3}. \quad (19)$$

Fig. 4 shows that a good correlation is obtained between the experimentally determined Nusselt number and the present calculation. The analysis is based on the Cebeci model and the new damping coefficient given by equation (19). In the subsequent analysis equation (19) is used.

Since it is difficult to make velocity measurement in flows of liquid metals, no experimental data is available. Therefore the predicted velocity distribution in the FD region is first verified with Laufer's experimental data [22] for air under the assumption of constant properties. On the other hand, the temperature measurement of temperature profile in flows of liquid metals is easier and vast data are available. Figure 5 shows the comparison of the calculated temperature profile for FD region (taken at $x/D = 44$) and the data obtained by Sleicher, Awad and Natter [18] for NaK. Figure 6 also compares the predicted T^{+} with data including sodium, Pb-Bi alloy, and mercury, compiled by Kirillov [21]. The correlation is good.

2. Developing thermal region (DT)

Before we present the calculations for the DT region it should be remarked that the damping constants A^{+} and B^{+} proposed by van Driest [2] and Cebeci [3] are

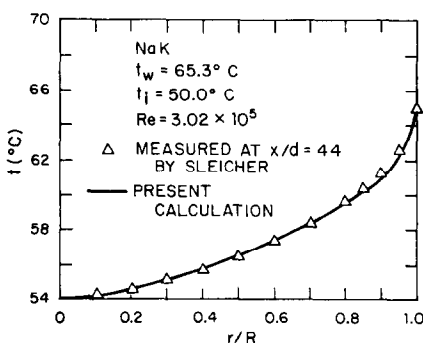


FIG. 5. Temperature profiles in fully-developed region.

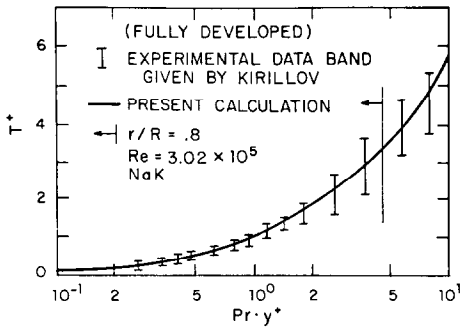


FIG. 6. Dimensionless temperature distribution in fully-developed region.

flow-dependent quantities. A^+ is known [26] to vary depending on whether the flow is under adverse or favorable pressure gradient and whether the flow is subjected to injection or suction. This suggests that the damping coefficient A^+ is a function of the flow geometry and boundary condition. A^+ is found to have a value of 26 for pipe flow. Similarly, the thermal damping constant B^+ is a function of the flow geometry and boundary condition. In the present investigation it is found that the thermal damping constant B^+ is a function of the Prandtl number as well as the flow region. Physically for liquid metals or fluids with small Prandtl numbers the thermal damping region becomes relatively large due to high molecular thermal diffusion. Thus the thermal damping region is likely affected by the local thermal boundary layer thickness. In other words, B^+ should depend on the growth of boundary layer thickness or enthalpy thick-

ness. We suggest the thermal damping constant for the developing regions to be

$$B^+ = B_x^+ \frac{\delta_T}{\delta_{Tx}} \quad \text{or} \quad 10.5 Pr^{-1/3} \frac{\delta_T}{\delta_{T\infty}} \quad (20)$$

That is, the thermal damping coefficient is proportional to the enthalpy boundary layer δ_T .

Figures 7 and 8 compare the predicted results for the developing thermal (DT) region and experimental data measured by Awad [19] under boundary conditions of constant wall temperature and constant wall heat flux. General agreement is obtained in both cases. Figure 7 in addition shows the results if the thermal damping constant B^+ does not take the local thermal boundary layer characteristic into account as given by equation (20). If instead equation (19) is used, the predicted results for the Nusselt number is smaller than in the experimental data of Awad.

From Figure 8 we find that the ratio of the local Nusselt number to the fully-developed Nusselt number, Nu_x/Nu_∞ , is not sensitive to changes of the Reynolds and the Prandtl except for the cases when the Peclet numbers are less than 5×10^2 . Since the plots of Nu_x/Nu_∞ vs x/D for various Reynolds numbers are similar, an approximate formula for Nu_x/Nu_∞ can be derived as follows:

$$\frac{Nu_x}{Nu_\infty} = 1 + \frac{2.4}{(x/D)} - \frac{1}{(x/D)^2} \quad x/D > 2 \text{ and } Pe > 500 \quad (21)$$

$$\frac{Nu_m}{Nu_\infty} = 1 + \frac{7}{(L/D)} + \frac{2.8}{(L/D)} \ln \left(\frac{L/D}{10} \right) \quad L/D > 2 \text{ } Pe > 500 \quad (22)$$

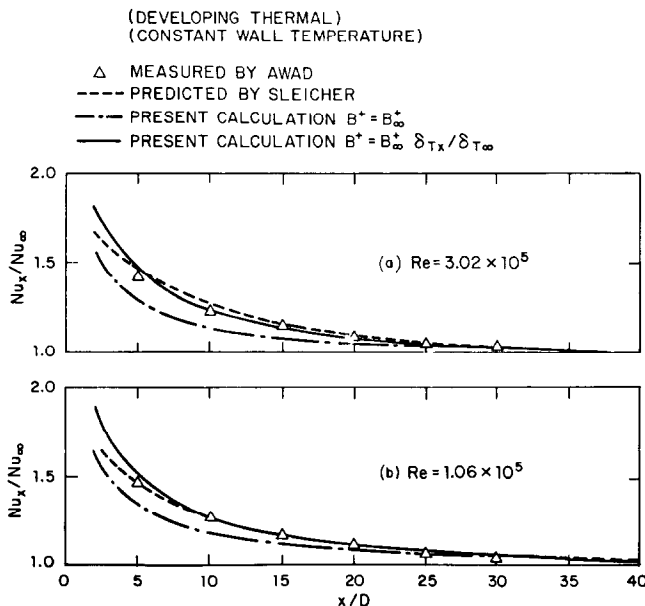


FIG. 7. Nusselt number in developing thermal region with constant wall temperature.

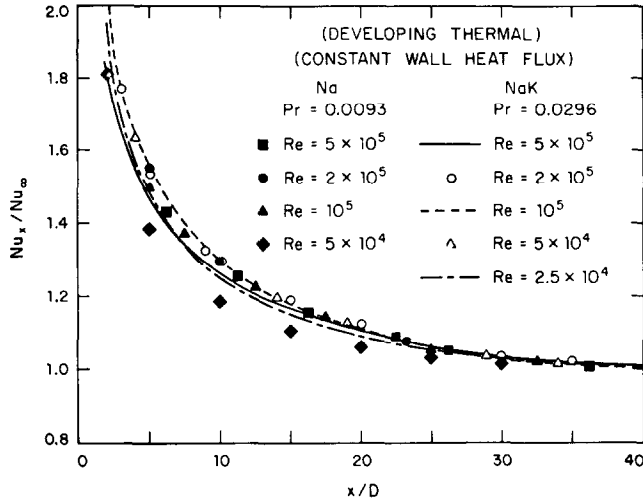


FIG. 8. Nusselt number in developing thermal region with constant wall heat flux.

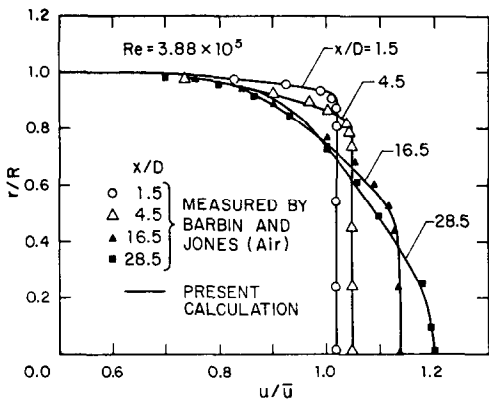


FIG. 9. Turbulent velocity distribution in the developing region.

$$Nu_{xc} = 5.6 + 0.0165 Pe^{0.85} Pr^{0.01}$$

for constant wall heat flux (23)

$$Nu_{xc} = 4.5 + 0.0156 Pe^{0.85} Pr^{0.01}$$

for constant wall temperature. (24)

Equation (21) is an improvement of Sleicher's formula given in equation (5). Equation (22) gives the average Nusselt number.

3. Developing thermal and velocity region (DTV)

Figure 9 compares the predicted velocity profiles at different axial locations with the data of Barbin and Jones [27] for $Re = 3.88 \times 10^5$. Agreement between the predicted profiles and measured data is obtained. It is found that the developing length for turbulent pipe flow is almost independent of the Reynolds number

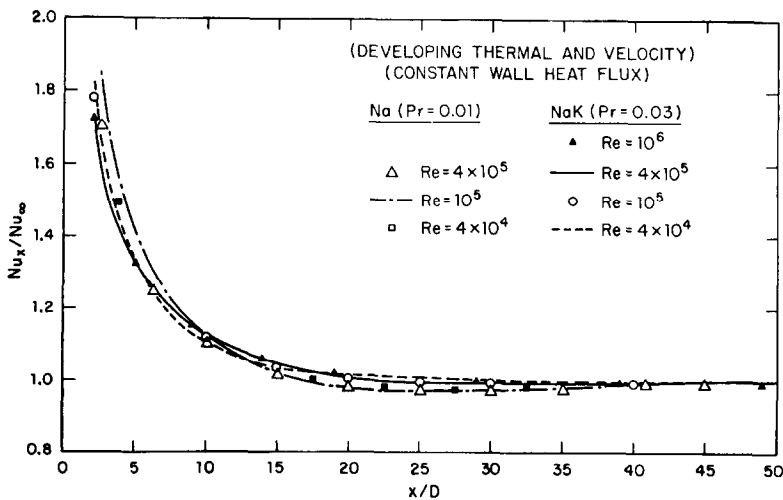


FIG. 10. Nusselt number in developing thermal and velocity region with constant wall heat flux.

and is about 35–50 diameters. The calculated Nu_x/Nu_∞ in the DTV region for all constant wall heat flux is given in Fig. 10. Again, since these plots are similar for the range of Reynolds numbers calculated they may be correlated in an approximated form

$$\frac{Nu_x}{Nu_\infty} = 0.88 + \frac{2.4}{(x/D)} - \frac{1.25}{(x/D)} - E \quad 2 \leq x/D < 35 \quad (25)$$

and for the mean Nusselt number Nu_m ,

$$\frac{Nu_m}{Nu_\infty} = 1 + \frac{5}{(L/D)} + \frac{1.86}{(L/D)} \ln \left(\frac{L/D}{10} \right) - F \quad (26)$$

Here for constant wall temperature it is found that

$$E = \frac{(40 - x/D)}{190}, \quad F = 0.09$$

and for constant wall heat flux

$$E = F = 0$$

Nu_∞ is given by equation (23) if the wall condition is constant heat flux and by equation (24) if the wall condition is isothermal.

4. Effect of variable properties

As the physical properties vary from fluid to fluid at different temperature ranges, it is impossible to describe the variation of fluid flow or heat transfer characteristics due to temperature change by a single relationship and to expect that the relationship will be valid for all fluids under all conditions. Instead, one has to calculate each fluid under the prescribed conditions. For design convenience, simple formulae that approximate the variation of friction coefficients or heat transfer coefficients are still favorable. Therefore in the present investigation the Nusselt number and friction coefficients are presented in the forms of

$$\frac{Nu}{Nu_0} = \left(\frac{T_b}{T_i} \right)^n \quad (27)$$

$$\frac{C_f}{C_{f0}} = \left(\frac{T_f}{T_i} \right)^m \quad (28)$$

where the subscript zero refers to the values calculated under the assumption of constant physical properties, T_b represents the bulk temperature, T_i is the inlet temperature, while $T_f = 1/2(T_b + T_w)$ is the film temperature. Details of the correlation are given by Chiou [28]; only results are summarized below.

(A) For sodium liquid, $m = -0.26$, and

(i) under constant wall heat flux

$$\begin{aligned} n &= \exp [5.9 \times 10^{-3} T_b - 6.91] \\ & \quad 1000\text{K} \geq T_b > 600\text{K} \text{ heating} \\ n &= 0 \quad 600\text{K} > T_b \geq 370\text{K} \text{ heating} \\ n &= 0.25 \quad \text{cooling} \end{aligned} \quad (29)$$

(ii) under constant wall temperature

$$\begin{aligned} n &= 0.08 + 2.2 \times 10^{-4} T_b \\ & \quad 1000\text{K} \geq T_b > 600\text{K} \text{ heating} \\ n &= 0.08 \quad 600\text{K} > T_b \geq 370\text{K} \text{ heating} \\ n &= 0.16 \quad \text{cooling} \end{aligned} \quad (30)$$

(B) For NaK eutectic, $m = -0.3$, and

(i) for constant wall heat flux

$$\begin{aligned} n &= -0.25 \quad \text{for heating} \\ n &= -0.15 \quad \text{for cooling} \end{aligned} \quad (31)$$

(ii) for constant wall temperature

$$n = -0.2 \quad \text{for heating and cooling.} \quad (32)$$

6. CONCLUSION

Liquid metal heat transfer in a circular pipe is investigated for both laminar and turbulent flows with constant wall temperature and constant wall heat flux as thermal boundary conditions. Three flow regions, namely the fully developed, developing thermal, and developing thermal and velocity regions, are considered. The modified mixing length model proposed by van Driest and Cebeci is adopted as the turbulence model for turbulent stress and heat flux. The thermal damping coefficient is redetermined to provide better prediction for liquid metal heat transfer in the developing region. Predicted velocity and temperature profiles and variation of the Nusselt numbers in three flow regions are verified with experimental data when available. Convenient approximate equations are derived from the predicted results for variation of the local Nusselt number in the developing regions. Furthermore, corrections for property variation are also given for liquid sodium and NaK eutectic.

REFERENCES

1. S. V. Patankar and D. B. Spalding, *Heat and Mass Transfer in Boundary Layers*, 2nd edn. International Textbook (1970).
2. E. R. van Driest, On turbulent flow near a wall, *J. Aero. Sci.* **23**, 1007 (1956).
3. T. Cebeci, A model for eddy conductivity and turbulent Prandtl number, *J. Heat Transfer* **C95**, 227–234 (1973).
4. R. Jenkins, Variation of the eddy conductivity with Prandtl modulus and its use in prediction of turbulent heat transfer coefficients. Proceedings on Heat Transfer Fluid Mechanics Institute, pp. 147–158. Stanford University (1951).
5. R. G. Deissler, Analysis of fully developed turbulent heat transfer at low Peclet numbers in smooth tubes with application to liquid metals. Research memo E52F09, NACA (1952).
6. N. E. Azer and B. T. Chao, A mechanism of turbulent heat transfer in liquid metals. *Int. J. Heat Mass Transfer* **3**, 121–138 (1960).
7. O. E. Dwyer, Eddy transport in liquid-metal heat transfer. *A.I.Ch.E.* **9**, 261–268 (1963).

8. T. Y. Na and I. S. Habib, Heat transfer in turbulent pipe flow based on a new mixing length model, *Appl. Sci. Res.* **28**, 302-314 (1973).
9. R. A. Baker and Alexander Sesonske, Heat transfer in sodium-potassium alloy, *Nucl. Sci. Engng* **13**, 282-288 (1962).
10. V. I. Subbotin, A. K. Papovyants, P. L. Kirillov, and N. N. Ivanovskii, A study of heat transfer to molten sodium in tubes, *Soviet J. Atomic Energy* **13**, 991-994 (1963).
11. V. M. Borishanskii and S. S. Kutateladze, Heat transfer and hydraulic resistance during flow of liquid metals in circular tubes, *Soviet Physics - Technology Physics* **3**, 781-791 (1958).
12. W. T. Sha and B. E. Launder, A general model for turbulent momentum and heat transport in liquid metals. Components Technology Division, Argonne, National Lab, Report number ANL-77-78 (1977).
13. P. L. Stephenson, A theoretical study of heat transfer in two-dimensional turbulent flow in a circular pipe and between parallel and diverging plates, *Int. J. Heat Mass Transfer* **19**, 413-423 (1976).
14. R. C. Martinelli, Heat transfer to molten metals, *Trans. ASME* **69**, 947-959 (1947).
15. R. L. Lyon, Liquid metal heat transfer coefficients, *Chem. Engng Prog.* **47**, 75-79 (1951).
16. B. Lubarsky and S. J. Kaufman, Review of experimental investigations of liquid metal heat transfer. NACA Report 1270 (1956).
17. O. E. Dwyer (editor), Heat transfer in liquid metals, in *Progress in Heat and Mass Transfer*, Vol. VII. Pergamon Press, Oxford (1973).
18. C. A. Sleicher, A. S. Awad, and R. H. Natter, Temperature and eddy diffusivity profiles in NaK, *Int. J. Heat Mass Transfer* **16**, 1565-1575 (1973).
19. A. S. Awad, Heat transfer and eddy diffusivity in NaK in a pipe at uniform wall temperature. Ph.D. dissertation, University of Washington, Seattle (1965).
20. O. J. Foust (editor), *Sodium-NaK Engineering Handbook*, Vol. 1. Gordon and Breach (1972).
21. P. L. Kirillov, Generalization of experimental data on heat transfer in molten metals, *Atomnaya Energrya* **13**, (1962).
22. W. M. Kays, Numerical solutions for laminar flow heat transfer in circular tubes, *Trans. ASME* **77**, 1265-1294 (1955).
23. W. M. Kays, *Convective Heat and Mass Transfer*. McGraw-Hill Series in Mechanical Engineering (1966).
24. C. A. Banston and D. M. McEligot, Turbulent and laminar heat transfer to gases with varying properties in the entry region of circular ducts, *Int. J. Heat Mass Transfer* **13**, 319-344 (1970).
25. R. K. McMordie and A. F. Emery, A numerical solution for laminar flow heat transfer in circular tubes with axial conduction and developing thermal and velocity field, *J. Heat Transfer* **89**, 11-16 (1967).
26. W. C. Reynolds, Computation of turbulent flows, *Annual Rev. Fluid. Mech.* **8**, 183-208 (1976).
27. A. R. Barbin and J. B. Jones, Turbulent flow in the inlet region of a smooth pipe, *J. Basic Engng* **85**, 29-34 (1963).
28. J. S. Chiou, Turbulent heat transfer in the pipe entrance region for liquid metals. Ph.D. dissertation, Energy Division, University of Iowa (1980).

TRANSFERT THERMIQUE LAMINAIRE OU TURBULENT A L'ENTREE D'UN TUBE POUR DES METAUX LIQUIDES

Résumé—On étudie le transfert thermique laminaire ou turbulent pour des métaux liquides en écoulement dans un tube. Trois régions sont considérées: pleinement développée, thermiquement développée, thermiquement et dynamiquement en développement. Les modèles de turbulence à longueur de mélange de Van Driest et de Cebeci sont adaptés pour cette analyse. La constante d'amortissement thermique est redéterminée dans la région pleinement développée aussi bien que pour les autres régions. Les résultats du calcul sont comparés avec les données expérimentales disponibles. Des formules sont données pour des conditions aux limites de flux thermique constant et de température pariétale isotherme. On étudie aussi l'effet de la variation des propriétés physiques. Une formule simple dans le cas de la propriété variable est donnée pour le sodium liquide et pour l'eutectique NaK.

WÄRMEÜBERGANG BEI LAMINARER UND TURBULENTER ROHRSTRÖMUNG IM ANLAUFGEbiet BEI FLÜSSIGEN METALLEN

Zusammenfassung—Es wird der Wärmeübergang von flüssigen Metallen bei laminarer und turbulenter Rohrströmung untersucht. Es werden drei Strömungsbereiche betrachtet, voll ausgebildete Strömung, thermischer Anlauf sowie thermischer und hydraulischer Anlauf. Das modifizierte Turbulenzmodell von van Driest und Cebeci für die Mischungsweglänge wird bei der Auswertung verwendet. Die thermische Dämpfungskonstante wird sowohl für voll ausgebildete Strömung als auch für noch nicht ausgebildete Strömungsgebiete bestimmt. Die berechneten Ergebnisse werden mit Meßwerten verglichen, soweit diese verfügbar sind. Gleichungen zur Wärmeübergangsberechnung werden für die Randbedingungen konstanter Wärmestromdichte und konstanter Wandtemperatur angegeben. Der Einfluß veränderlicher physikalischer Eigenschaften wird auch betrachtet. Eine Beziehung für den Wärmeübergang bei variablen Stoffwerten kann in einfacher Form für flüssiges Natrium und eutektisches NaK angegeben werden.

ЛАМИНАРНЫЙ И ТУРБУЛЕНТНЫЙ ПЕРЕНОС ТЕПЛА НА НАЧАЛЬНОМ УЧАСТКЕ ТРУБЫ ПРИ ТЕЧЕНИИ ЖИДКИХ МЕТАЛЛОВ

Аннотация — Исследуется ламинарный и турбулентный перенос тепла при течении в трубе жидких металлов. Рассматриваются три области течения, а именно: полностью развитая область, область развития теплового пограничного слоя и область развития теплового и динамического пограничного слоя. При анализе используется модифицированная модель длины смещения Ван Дриста и Чебечи. Дано новое определение коэффициента теплового сопротивления для всех областей. Результаты расчета сравниваются с имеющимися экспериментальными данными. Приведены соотношения для расчета теплопереноса как при постоянном тепловом потоке, так и при постоянной температуре стенки. Исследуется также влияние изменения физических параметров. Обобщенная зависимость для расчета теплопереноса при переменных параметрах дана в простой форме для жидкого натрия и эвтектики NaK.